84-2508

ASAE TECHNICAL
PAPER NO.

FACTORS INFLUENCING INFILTRATION FLOW INSTABILITY AND MOVEMENT OF TOXICS IN LAYERED SANDY SOILS

by

Robert J. Glass, Graduate Research Assistant
and
Tammo S. Steenhuis, Associate Professor

Department of Agricultural Engineering
Cornell University
Ithaca, N.Y.
14853

For presentation at the 1984 winter Meeting
AMERICAN SOCIETY OF AGRICULTURAL ENGINEERS

Hyatt Regency
New Orleans, LA
December 11-14, 1984

SUMMARY: The main findings of this research into unstable wetting fronts in two-layer sand systems where a fine layer overlies a coarse layer are that high initial moisture contents allow instability to occur, that unstable flow fields change very little in time even over relatively long lengths of time, and that properties of instabilities or fingers may be systematically explored through controlled laboratory experimentation.

American Society of Agricultural Engineers

St. Joseph, Michigan 49085

FACTORS INFLUENCING INFILTRATION FLOW INSTABILITY AND MOVEMENT OF TOXICS IN LAYERED SANDY SOILS

Robert J. Glass and Tammo S. Steenhuis

INTRODUCTION

Over the past twenty to thirty years the application of solute transport theory based on laboratory soil column experiments to field situations has been less than successful. There is a growing realization that the piston type flow observed in laboratory columns (Bodman and Coleman, 1943) does not adequately describe field solute transport. This should not be surprising as more than a century ago, Lawes et al. (1882) found that a large portion of water added to a soil only slightly interacted with that already present in the root zone. Yet, the piston flow model still forms the basis of conventional models currently in use (see Thomas and Phillips, 1979).

At present, research on nonpiston type heterogeneous flow can be divided into two general approaches: statistical and phenomenological. The statistical approach superimposes on the piston flow model a distribution of solute travel times obtained from intensive random sampling of an individual field. This approach will yield a good prediction of the transport of pollutants to the water table under a particular field but intensive sampling must be done for each field in question, a time consuming and expensive undertaking.

The phenomenological approach consists of defining and describing mechanisms that cause heterogeneous flow. Two mechanisms have been determined, that involving movement in isolated channels of high hydraulic conductivity or through macropores (eq., Dixon and Peterson, 1971; Ehlers, 1975; Elrick and French, 1966; Thomas et al., 1973; Germann and Beven, 1981; Russo and Bresler, 1981; Quisenberry and Phillips, 1976) and that due to wetting front instability also termed infiltration flow instability or "fingering."

Current field and laboratory evidence (Hill and Parlange, 1972; Starr et al., 1977; Diment, 1982) has shown that for soils whose hydraulic conductivity increases with depth but does not vary from point to point horizontally, wetting front instability can cause non-uniform solute transport. In these soils, water and toxics can move in preferred paths to groundwater at speeds approaching the saturated hydraulic conductivity of the subsoil.

Wetting front instability, however, is not fully understood and the importance of wetting front instability for field situations cannot be adequately assessed. If the work of Parlange and Hill (1976) and

Philip (1975a) is correct then the phenomenon is widespread. Parlange and Hill (1972) state that "among the several thousand soil series in the United States, there are about 350 series in family groups . . . (that) should be unstable." If Diment (1982) is correct, then the phenomenon is restricted to coarse dry sands which under some initial moisture conditions would still remain stable. Experimental field work of Starr et al. (1978), however, indicates the phenomenon to occur in situations that Diment's analysis would indicate are stable.

It is the purpose of this study to further the understanding of the wetting front instability phenomenon through systematic quantitative laboratory experimentation.

EXPERIMENTAL DESIGN

Two laboratory experimental sets, A and B, were formulated. Experimental set A was designed to determine the effect of a) the mean grain size of the porous medium layers and b) the initial moisture content of the system, both degree and distribution, on flow field behavior. The flow field behavior was characterized by whether the wetting front was unstable or stable, and if unstable, the number, width, spacing, velocity, discharge, merger and splitting of fingers. In addition, the influence of contact angle was demonstrated by comparison with two experiments (Pre2 and Pre3) conducted on sand before it was subjected to the cleaning process described below (pre-cleaned sand). The objective of experimental set B, or point source experiments was to explore the lateral movement of water from an isolated finger into the surrounding dry porous media.

EXPERIMENTAL SET A DESCRIPTION

In experimental set A, distilled water with a constant low non-adsorbing dye concentration (.025% solution of USDA Red #3) of constant temperature (20°C) gave constant fluid density and viscosity. The porous medium was composed of quartz sand with low impurity either in quartz grain chemical composition or by grains of minerals other than quartz. This sand purity, a cleaning procedure and the constance of the fluid properties assures the variation in contact angle to be the smallest possible.

A two dimensional flow field was explored due to ease of visual observation and documentation. Since the width of all fingers in any of the sands was greater than 1 cm, the space between the walls (depth) of the slab infiltration chamber (described in detail below) was held at 1 cm to force a two dimensional flow field. The width of the chamber was held at 30 cm. The height of the bottom layer was kept at 81 cm and that of the top layer above at 13 cm for experiments A1 to A2 and at 8 cm for experiments A5 to A9. Variations in these heights never exceeded 1 cm. The interface geometry was made as flat and free of spatial perturbations as possible thus approximating the random infinitesimal perturbations assumed in hydrodynamic stability analysis.

Water was applied to the top of the system by ponding to a depth of 1.5 cm quickly, usually within 10 sec., and maintained this depth throughout the duration of each experiment.

The microscopic length scale of the porous medium was varied systematically through the use of sands of differing mean grain size with narrow and approximately the same log scale grain size distribution (see Table 1). These sands allowed systematic variation in the composite variables of conductivity, moisture characteristic relation, diffusivity and sorptivity. The sand used for the bottom layers always had a greater mean grain size than the sand used for the top layers to insure $K_{bot} > K_{top}$.

The initial moisture content degree and distribution were varied systematically in experiments A6 through A9 by running three consecutive experiments in each experimental porous media packing. In the first experiment, denoted by a lower case "a", the media was dry everywhere with essentially no moisture present (oven dried sand). This experiment was allowed to continue for twenty-four hours and then drained for twenty-four hours. The heterogeneous moisture content field at the end of the drainage cycle was the initial field for the second experiment, denoted by a lower case "b", which was also conducted for twenty-four hours. The bottom layer was then saturated by means of ports through the slab chamber wall at the top of the bottom layer and allowed to drain for another twenty-four hours. This homogeneous moisture field (6%) in the bottom layer formed the initial moisture field for the third experiment denoted by a lower case "c". In this way a heterogeneous initial moisture content field representative of nature was simulated in the second experiment while the first and third experiments represented more extreme naturally occurring initial moisture content fields which satisfy conditions used in analytical and numerical studies of infiltration flows.

In the last three experiments (Ababc, A8abc and A9abc), the flux out the bottom of the chamber was measured through 10 drip sections each having a width of 3 cm. This enabled the monitoring of the flux through individual fingers and its change in time. Measurements were taken at least at two occasions, within one hour and after 24 hours from the start of ponding.

EXPERIMENTAL SET B

Individual fingers were simulated by removing the top fine layer and applying a known flux of water directly on the top of the porous medium from a burett as a point source. This procedure both yielded the same structure as a finger and mimicked the hypothesized nature of the textural interface as a distribution of point sources. Thus, the flow field was simplified allowing the properties of a single finger to be explored. An analogous simplification technique was used in saturated flow by Saffman and Taylor (1958) to generate one finger in a Hele-Shaw cell.

The effect of initial moisture content was also examined by running experiments at two uniform moisture contents: completely dry and after saturation and drainage for 24 hours which yielded a moisture content of 6%. Six experiments were conducted. Fluxes of 10, 20 and 30 ml/min were supplied to the top of a layer of 14-20 sand at the two uniform initial moisture contents, completely dry and 6% (see Table 1).

LABORATORY EXPERIMENTAL APPARATUS AND PROCEDURES

Sand Preparation Procedure: Sieving and Cleaning

White silica sand used commercially for sand blasting was dry sieved through a nesting sequence of 8-inch wire mesh sieves (US sieve series numbers 14, 20, 30, 40, 50, 60, 80, 100, 140, 200) by a mechanical shaker. Six of these sand fractions were used as the experimental sands constituting a porous media layer (see Table 1).

Table 1. Prepared Sands

US Sieve Series #'s	Maximum and Minimum Diameter (mm)	Mean Grain Diameter (mm)	Ln** Diameter spread	Saturated* Hydraulic Conductivity K_s (cm/min)
140-200	.105-.074	.088	.350	.8
100-140	.149-.105	.125	.350	1.3
60- 80	.250-.177	.210	.345	1.8
40- 50	.420-.297	.272	.347	6.9
20- 30	.841-.595	.707	.346	22.4
14- 20	1.168-.841	.991	.329	42.5

*measured at a porosity of 42%.
**natural log of maximum diameter minus natural log of minimum diameter

The sands obtained from dry sieving were cleaned to assure uniform contact angle across all the sands. Each sand was boiled in a .5% solution of Pex laboratory glass cleanser used for analytical and research laboratory glassware for 1/2 - 3/4 hours. The sand was then rinsed with warm tap water 15 times with noticeable effects of the soap disappearing by the 5th to 8th rinse. Next, the sand was boiled in tap water for 15 minutes and rinsed an additional three times to assure the removal of all soap.

Small portions of the sand were then placed on the finer sieve (cleaned with the same procedure as the sand) defining the lower end of the sand fraction and wet sieved for one minute. This allowed additional rinsing and the removal of any dust and finer particles that the dry sieving could have missed. The sand was then rinsed five times with distilled water and allowed to dry in aluminum trays in a drying oven at 60-70°C for a week. Finally, the dry sand was stored in plastic buckets with lids to insure against contamination from air borne particles.

Two Dimensional Slab Infiltration Chamber

The two dimensional slab infiltration chamber was designed with the following specifications: variable width; variable depth (to force 2-D flow); variable height; and clear to allow photographic documentation. The chamber was constructed out of half-inch thick clear Plexiglass and made in sections which stacked in a frame (see Figure 1). In this way the height of the chamber could be varied by the number of sections stacked upon each other. The width could be varied by moving the width spacer or removing it entirely giving a maximum width of 51 cm. The depth could be varied by replacing the spacers on either end or in the middle with others of the desired depth.

In early experiments the bottom piece on which the sections are stacked had holes drilled in it to allow air and water to flow out of the chamber and was covered by a 120 mesh screen to keep sand from falling through the holes. In later experiments (from A6 - A9) a bottom drip section was constructed so that the flow through individual fingers could be monitored. The bottom 30 cm wide slab section was divided into 10 drip sections of 3 cm each. A hole in the bottom of each drip section was connected to a tube allowing the water to flow into graduated cylinders.

Filling Apparatus

It was found that horizontal homogeneities in the pack could only be eliminated by pouring the sand such that the sand level in the chamber rose evenly across its width. To do this, a slotted two-dimensional funnel was constructed. Across the slot was placed triangular barriers within which holes were drilled to allow sand to escape, the number and spacing of the holes were varied depending on the grain size of the sand being poured through the funnel. This funnel was attached to the top of a 68 cm extension that fit above the slab chamber. The extension contained a wide wire mesh grate 10 cm from the bottom that acted as a falling sand randomizer. The combination of many openings of the same diameter equally spaced across the top of the extension and the randomizer at the bottom yielded the desired horizontally even fill.

Packing Apparatus

The sand slab once filled was packed with a simple drop packing method. The slab chamber and frame was raised up 3/4" and dropped back onto the platform repetitively until the desired number of drops had occurred (200 drops). To achieve this a special "dropper" was designed. The dropper raised the chamber at its base through the rotation of two shafts each having two widely spaced half-moon cams riding on metal stock bolted to the bottom of the chamber frame. The two cam shafts were linked by a chain to a small Dayton Gearmotor that provided the necessary lifting force. The chamber frame was stabilized at the top by two, two-inch pipes that ran from floor to ceiling. After packing, at least the top 10 cm of sand overburden was removed as this was found to have a lower bulk density than below.

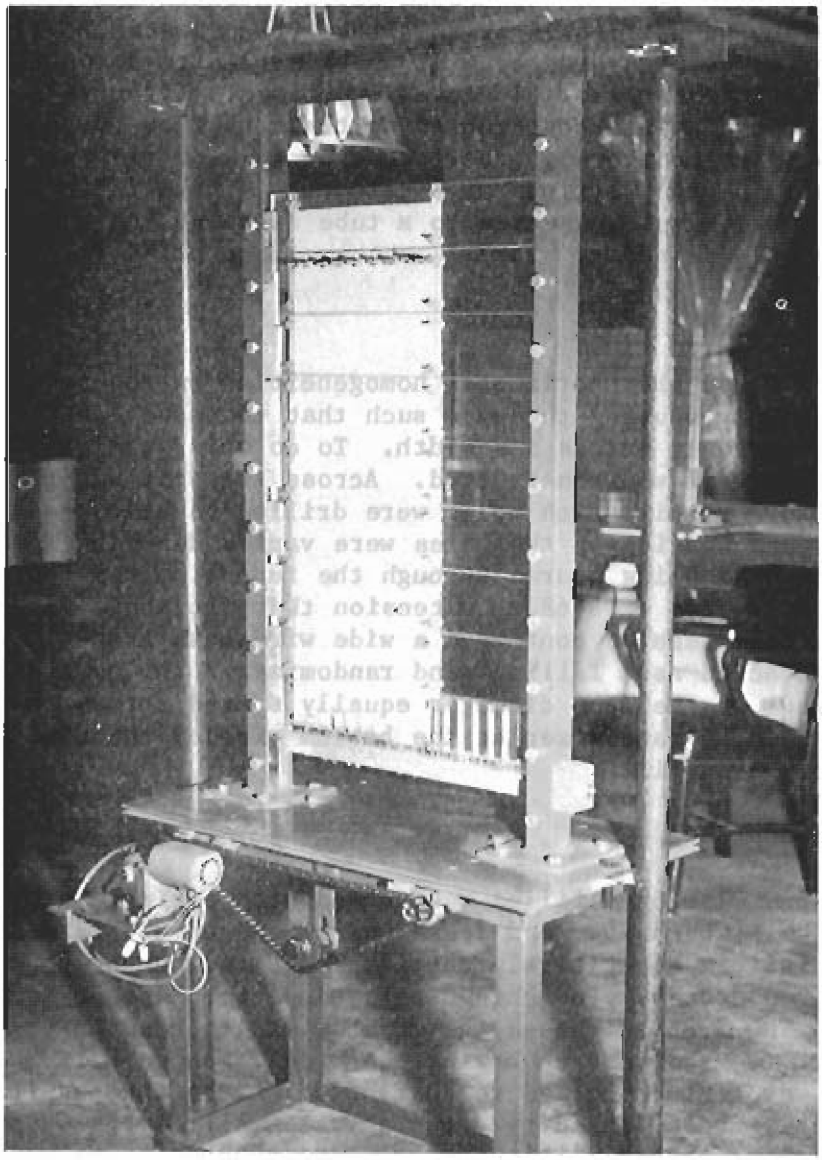

Figure 1. Photograph of laboratory experimental apparatus.

Fluid Application System and Application Procedure

In the two layer ponded experiments, fluid was applied evenly across the top of the porous media through a plastic pipe containing many small holes (approximately one each cm) to insure a flat wetting front through the top layer. A constant flux master flex pump applied fluid to the plastic pipe, its rate controlled by a variable voltage transformer. The depth of ponding was maintained constant by a take-off tube that was connected back to the pump.

In the point source experiments, fluid was applied to the mid-point at the top of the porous media from a 50 ml burette. A constant flux was achieved by maintaining a constant fluid level in the burette with a constant head mariott device.

Flow Field Data Recording System

Flow field data were recorded with a Bolex movie camera set to take a frame every 2.5 seconds. Data was pulled from the film by projecting it onto a screen and then tracing the wetting front position with time on acetate sheets. Finger widths were pulled from the tracings by determining the area of the finger over a 15 to 20 cm length near the bottom of the chamber. In this way the width was averaged as finger edges tended to be bumpy and were never exactly flat. Finger velocities and dye velocities were pulled directly from the movie film.

PRESENTATION AND DISCUSSION OF RESULTS

EXPERIMENTAL SET A - TWO LAYER EXPERIMENTS

Tables 2 and 3 give the results of the two layer experiments outlined above. Table 2 gives the experiment number, bottom and top layer combination, porosity, thickness of the top layer, initial moisture content conditions, flux through the system during the early part of the experiment, whether it was stable or unstable, and the run time of the experiment. Table 3 gives for the experiments where the porous medium was initially dry ("a" experiments), the number of fingers that formed under the textural interface (initial), the number of fingers that continued to the bottom of the apparatus (final), the maximum, minimum and average width and velocity of the fingers (excluding fingers that ran down the edge of the chamber), and the percent of the total width of the chamber occupied by fingers. Finger velocity refers to the velocity of the finger tip as it advances downward through the porous medium.

Figure 2 is a drawing of the wetting front position at time increments of one minute in experiment A6a. As is designated in Table 2, A6a was a two layer experiment with a top layer of 100-140 sieve fraction sand and a bottom layer of 14-20 sand conducted under uniform dry initial moisture content conditions. As is shown in Figure 2a, at the end of the first minute, the wetting front has moved across the textural interface at discrete locations which will be referred to as "point sources". Figures 2b to 2e show the growth of fingers from the

Table 2. Summary Table Two Layer Experiments

Run	Bottom Layer Sand	Porosity	Top Layer Sand	Thickness Top Layer (cm)	Initial θ Conditions	Initial Q through System (cm/min)	Stable or Unstable	Run Time of Experiments (hrs)
A6a	14-20	.42	100-140	8.0	Dry	1.95	Unstable	24
A6b					1 day drainage of A6a	1.66	Unstable	24
A6c					Saturation then 1 day drainage	1.27	Marginally Unstable	24
A9a	14-20	.42	60-80	8.0	Dry	4.15	Unstable	24
A9b					1 day drainage of A9a	3.45	Unstable	24
A9c					Saturation then 1 day drainage	4.88	Marginally Unstable	24
A8a	14-20	.42	40-50	8.0	Dry	11.97	Unstable	24
A8b					1 day drainage of A8a	7.10	Unstable	24
A8c					Saturation then 1 day drainage	2.26	Marginally Unstable	24

Table 2. Summary Table Two Layer Experiments (continued)

Run	Bottom Layer Sand	Porosity	Top Layer Sand	Thickness Top Layer (cm)	Initial θ Conditions	Initial Q through System (cm/min)	Stable or Unstable	Run Time of Experiments (hrs)
Pre2*	14-20	.43	30-40	15.75	Dry	19.5	Unstable	.17
A5a	20-30	.42	100-140	8.5	Dry	1.27	Unstable	5
A7a	40-50	.41	100-140	8.0	Dry	1.62	Unstable	24
A2	40-50	.41	60-80	13.0	Dry	4.17	Unstable	.25
Pre3*	40-50	.42	60-80	15.3	Dry	4.0	Unstable	.17
A1	60-80	.42	140-200	13.0	Dry	1.23	Marginally Unstable	.5

*Experiments conducted with pre-cleaned sand

Table 3. Summary Table Initially Dry Two Layer Experiments

Run	Number Initial Fingers	Number Final Fingers	Max. Finger Width (cm)	Min. Finger Width (cm)	Average Finger Width (cm/min)	Max. Finger Velocity (cm/min)	Min. Finger Velocity (cm/min)	Average Finger Velocity (cm/min)	% Total Width Occupied By Fingers
A6a	10	5	1.78	1.12	1.52 ± .28	30.45	18.63	25.1 ± 5.1	25
A9a	13	6	2.11	1.33	1.67 ± .40	43.6	26.9	35.0 ± 7.6	33
A8a	13	5	3.45	3.15	3.31 ± .15	58.3	54.1	56.1 ± 1.49	53
Pre2*	12	5	3.1	.89	2.12 ± 1.0	71.9	40.4	57.7 ± 14.7	35
A5a	9	5	3.51	1.4	2.29 ± .85	20.3	9.5	15.24 ± 5.24	38
A7a	5	3	--	--	12.7**	--	--	10.42**	62
A2	3	3	--	--	20.7**	--	--	11.8**	100
Pre3*	12	8	3.85	1.18	2.13 ± .96	14.0	9.1	12.1 ± 1.6	57

*Experiments conducted with pre-cleaned sand
**Only one finger observed that did not run down the edges of the chamber

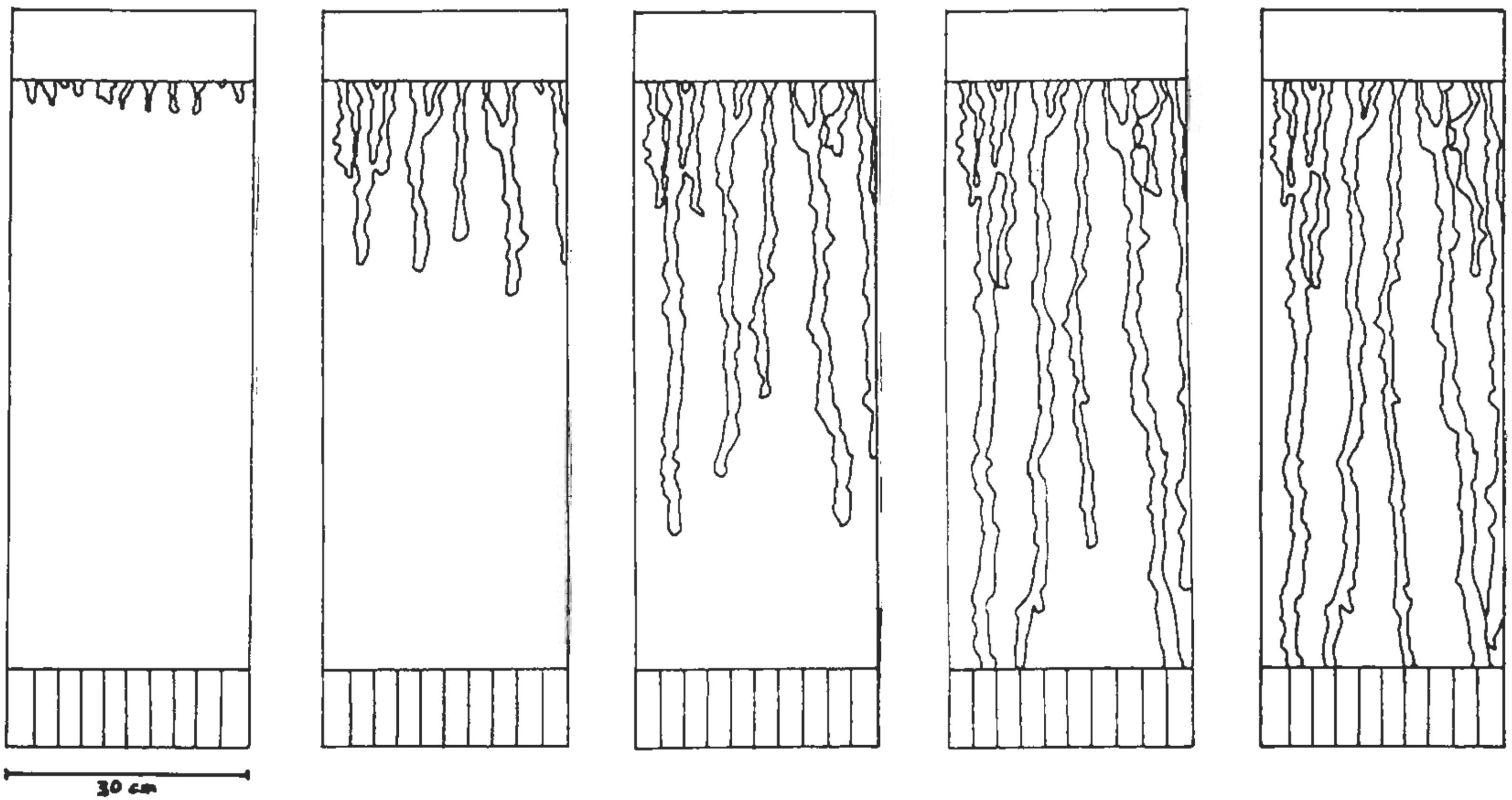

a) 1 min   b) 2 min   c) 3 min   d) 4 min   e) 5 min

Figure 2. Experiment A6a. Wetting front position for time intervals of one minute after the start of infiltration into an initially dry, two layer sand system.

individual point sources after 2, 3, 4, and 5 minutes respectively. The information of Figures 2 may be condensed into a composite drawing shown in Figure 3.

Qualitative Description of Two Layer, Unstable Flow Field

Experimental set A has yielded the following composite qualitative description of the unstable flow field in the two layer sand system with K_{top} less than K_{bot}.

For infiltration into initially dry two layer sand systems ("a" experiments), the unstable flow field may be divided into four zones: the top layer, the interface between the two layers, the "induction" zone and the fully developed finger zone (see Figure 3). Flow in the finer top layer is characterized by an initially flat wetting front and vertical streamlines. The interface between the two layers seems to act as a discretizer of the uniform flow in the top layer allowing water to pass into the bottom layer at discrete, fairly regularly placed locations or "point sources." The induction zone extends from the interface to from 6 to 10 cm below. In this zone water "threads" from the point sources at the interface coalesce into fingers and then some fingers merge to form wider fingers. These fingers then pass into the fully developed finger zone which is characterized by fairly constant finger velocity, width and spacing. Occasionally in this zone merger of fingers will occur to produce a faster moving wider finger.

Three periods in the development of the flow field in the initially dry case may be delineated a) an initial "rapid" period, b) a transitional "slow" period and c) a final period of almost no change.

The initial "rapid" period is characterized by rapid change in wetting front position with time and is shown in Figure 3 for experiment A6a. It continues until the descending fingers arrive at the water table or, in the case of the laboratory experiments conducted in the slab chamber, when they arrive at the bottom of the chamber and create a water table (water will drip out the bottom of the chamber when the water table height has reached that of the capillary rise).

The transitional "slow" period is characterized by very slow changes in wetting front position as wetting fronts move laterally into the dry areas between fingers. This period is shown in Figure 4 for experiment A6a. The diffusing water creates a less saturated fringe around the more saturated core areas defined by the initial location of the fingers in the dry porous medium. Most of the flux in the system occurs downward in these core areas and is due to the influence of gravity. The movement in the fringe areas is caused by both pressure gradients due to moisture content variations (mostly lateral) and by gravity. Occasionally during this period a finger itself will become unstable and a small split-off finger or "dendrite" may form and move slowly downward to the water table. The period ends when the lateral wetting fronts have moved through all the porous media and some moisture is present at all locations. This may take some time (e.g., several days) before all the porous medium is moist and it is important to note that moisture content drops dramatically outside of any of the initial finger limits which constitute finger core areas.

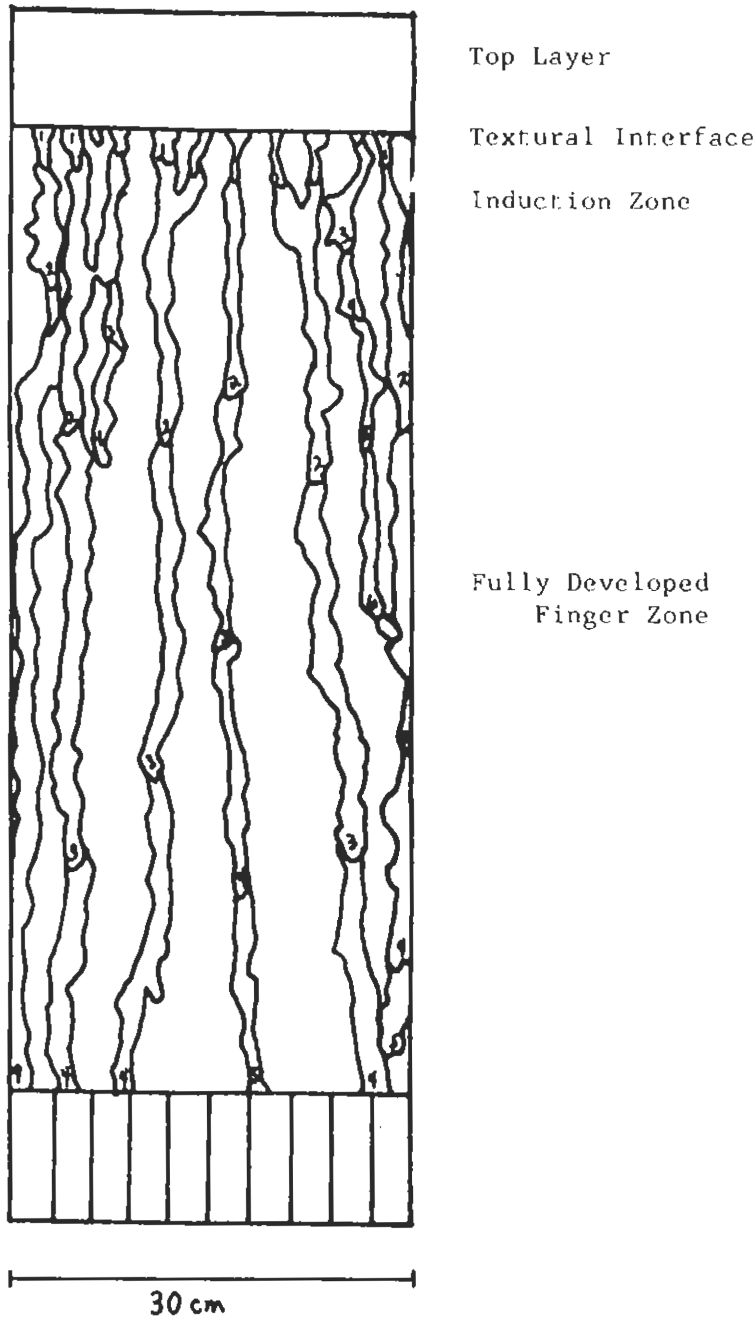

Figure 3. Composite drawing of experiment A6a. Wetting front position for time intervals of one minute after the start of infiltration into an initially dry, two layer sand system.

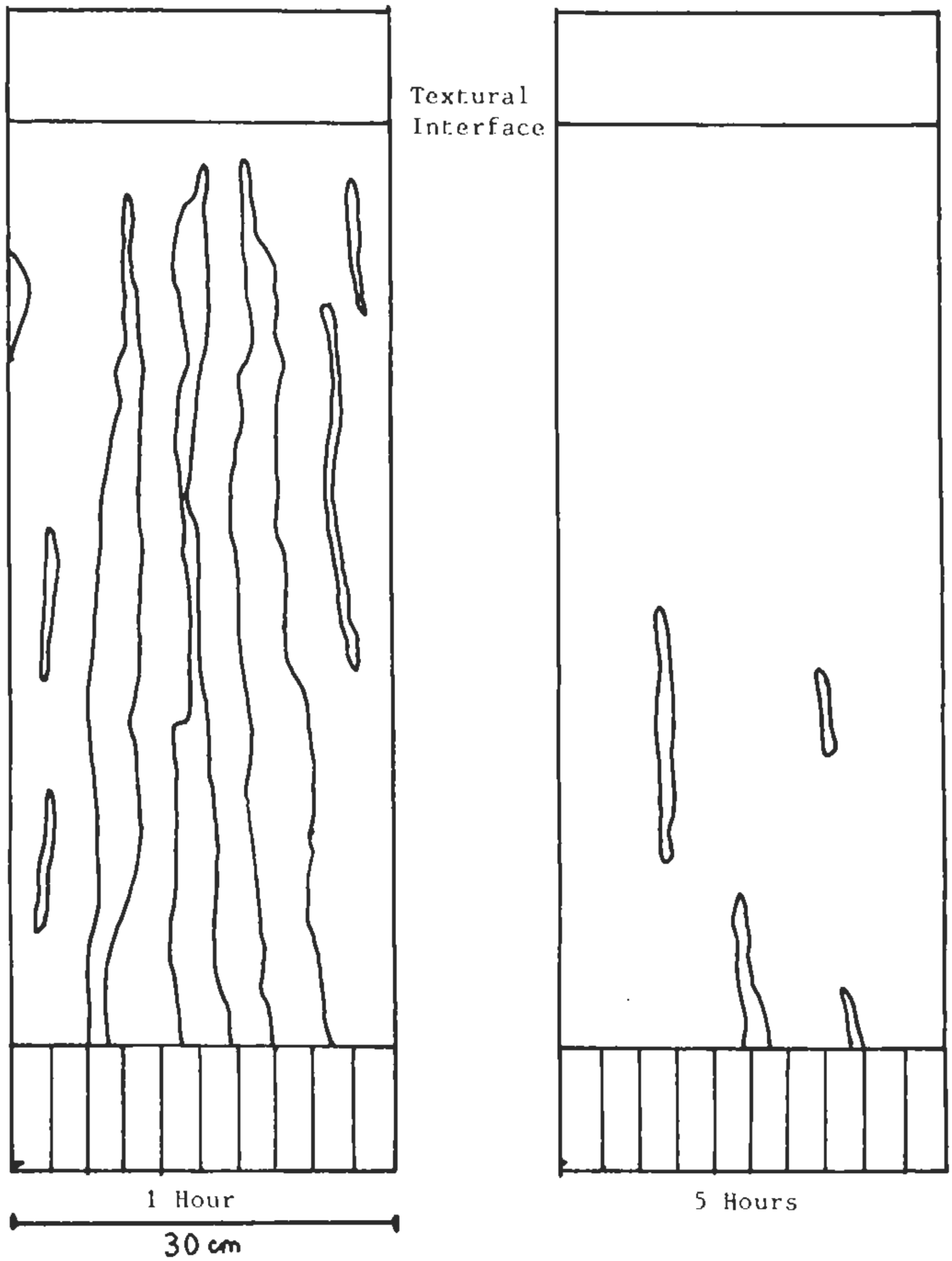

Figure 4. Experiment A6a. Wetting front position drawn for transitional "slow" period where wetting fronts move laterally into dry areas between fingers.

The final period is characterized by no visual change in flow field direction or magnitude. In this period the fully developed "unstable" field has become the new base or primary flow field. Large moisture content differences are visible between the core areas and the fringe areas but lateral pressure gradients due to these differences have become insufficient to cause any further lateral movement of water. All movement is due to gravity and is in the downward direction. This period has been documented to last for at least 10 days, the longest duration of any of the experiments, and may well last indefinitely.

In the "b" experiments performed on a packing with a heterogeneously distributed initial moisture content left after drainage of the experiment on the initially dry sand, fingers form in the same locations as in the "a" experiments. This can be seen in Figure 5, the composite drawing of experiment A6b. Movement in the former fringe areas is enhanced giving the fingers the appearance of greater width but the size and configuration of the core area match almost exactly with that of the previous initially dry experiment. The velocities of the finger tips are less than in the previous dry experiment due to the participation of the fringe areas in conducting water and thus lowering the moisture content in the core areas. Basically, this heterogeneous initial moisture content field allows a rapid transition into the third and final flow period by enhancing movement in the fringe areas.

The description of the flow field given for the dry experiments also corresponds to that for the heterogeneous initial content experiments. All four zones are present as indicated by dye tracer studies. The only difference is a slight movement across the textural interface in between the initial point sources as evidenced by dye tracer pulses.

In the final experiment run on a packing, "c" experiments, the moisture content in the bottom layer is at a uniform homogeneous level of approximately 6%. The wetting front as it moves into the bottom coarse layer becomes wavy and the amplitude of the wave increases as the wetting front proceeds downward. This is exemplified in Figure 6, the composite drawing of experiment A6c. Thus, the wetting front is indeed unstable. However, the dramatic finger structure found in the dry and heterogeneous distribution experiments is not observed initially and does not develop over time. Likewise, the zones shown in Figure 3 are not apparent nor can any time periods be distinguished.

<u>Influence of Initial Total Flux through the Initially Dry Two Layer System</u>

The initial total flux Q_T, through the two-layer system is controlled by the conductivity and height of the top finer layer. Contrary to the findings of Hill and Parlange (1972), experiments A6a through A9a demonstrate that the total flux, Q_T, through the system varying from 1.95 to 11.97 cm/min influences the number of fingers only slightly.

Also contrary to their findings, finger velocity is effected markedly by total flux through the system. Maximum, minimum and

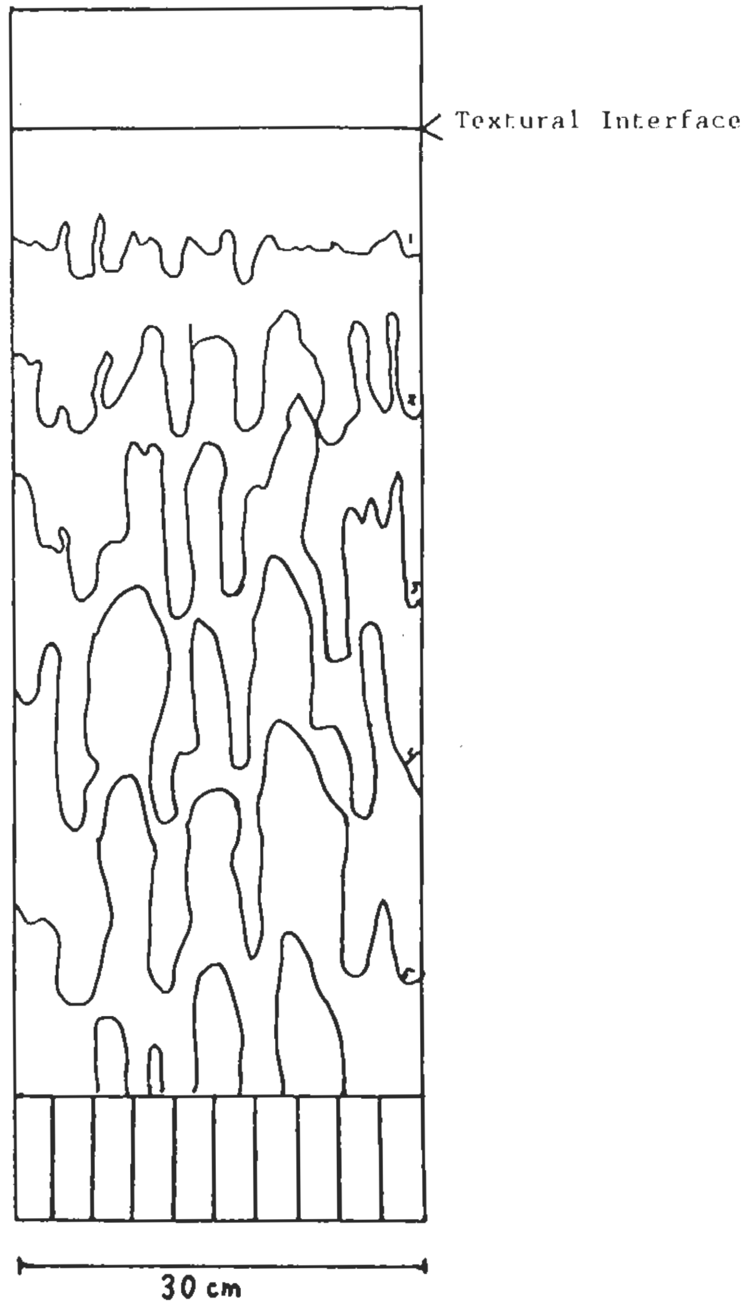

Figure 5. Composite drawing of experiment A6b. Wetting front position for time intervals of one minute after the start of infiltration, initial moisture content field was heterogeneously distributed as generated by the previous experiment A6a.

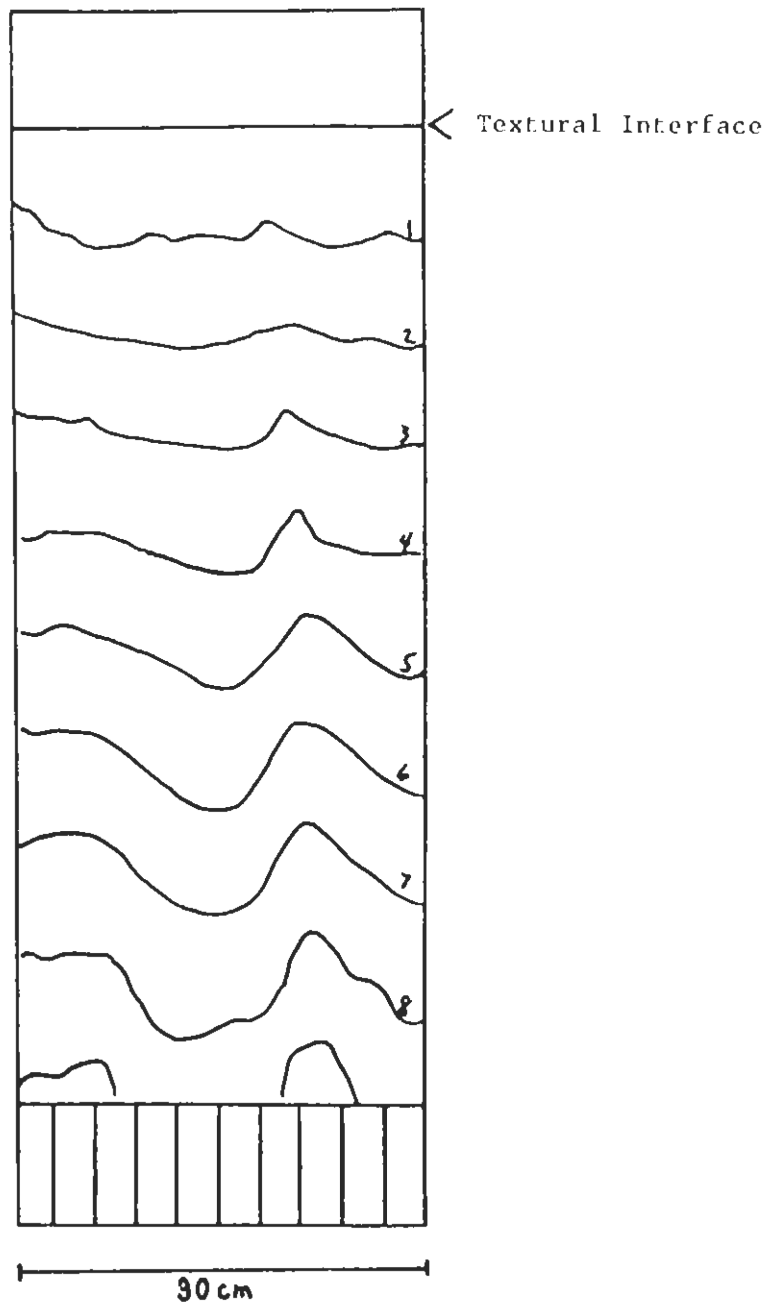

Figure 6. Composite drawing of experiment A6c. Wetting front position for time intervals of one minute after the start of infiltration, initial moisture content of 6% (field capacity) distributed evenly through the two layer sand system after A6b.

average finger velocities all increase with Q_T. A plot of average finger velocity ± standard deviation versus Q_T is given in Figure 7. This shows that the influence of Q_T on the finger velocity is much greater at low Q_T than at high Q_T; i.e., small increases in Q_T lead to large changes in average finger velocity at low Q_T while at high Q_T, a large change yields small changes in average velocity. The maximum finger velocity possible is given by the saturated conductivity, K_s, of the porous media divided by its porosity or approximately 101 cm/min for the 14-20 sand. While this velocity may be achieved by a finger, it certainly will be achieved when Q_T is the same as K_s and the chamber (42.5 cm/min) is completely filled with one "finger" - the stable situation. Thus it is hypothesized that the curve in Figure 7 may be extended out smoothly to this point.

The effect of the total flux on width is not very important at lower fluxes as evidenced by experiment A6a and A9a. The average finger width in these runs are very nearly the same. The increase in total flux from 4.25 to 11.97 cm/min, however, brings a doubling in average width from 1.67 ± .4 to 3.31 ± .15 cm. Figure 8 is a plot of average width ± standard deviation versus Q_T and shows this sensitivity of finger width to Q_T for high Q_T.

The number of fingers and their widths are combined to give the percentage of chamber width occupied by fingers. This percentage is seen in Table 3 to increase as expected.

EXPERIMENTAL SET B - POINT SOURCE EXPERIMENTS

Summary Table 4 gives the results of the point source experiments. For the prescribed flux, Q_f, and initial moisture conditions, the width, and finger wetting front velocity are recorded. Composite drawings of experiments D6 and D3 where Q_f was 20 ml/min are shown in Figures 9a and 9b.

Qualitative Description of Point Source Experiments

In the initially dry experiments, single fingers generated by the point source at the top of the coarse layer are qualitatively identical to those that occur in the initially dry two layered experiments (see Figure 9a). The three stages in flow field development are present, the second stage lasting longer due to much larger space between "fingers", i.e., between the fingers and the walls. Core areas are well defined and the widening of the fringe areas can be seen to be due to both lateral and downward movement within the fringe areas. Downward moving bulges that occasionally develop into dendrites are present in all runs indicating the importance of gravity on movement within the fringe areas. These dendrites also point to the marginal stability of the flow within the fringe region where the flux is much less than the saturated conductivity.

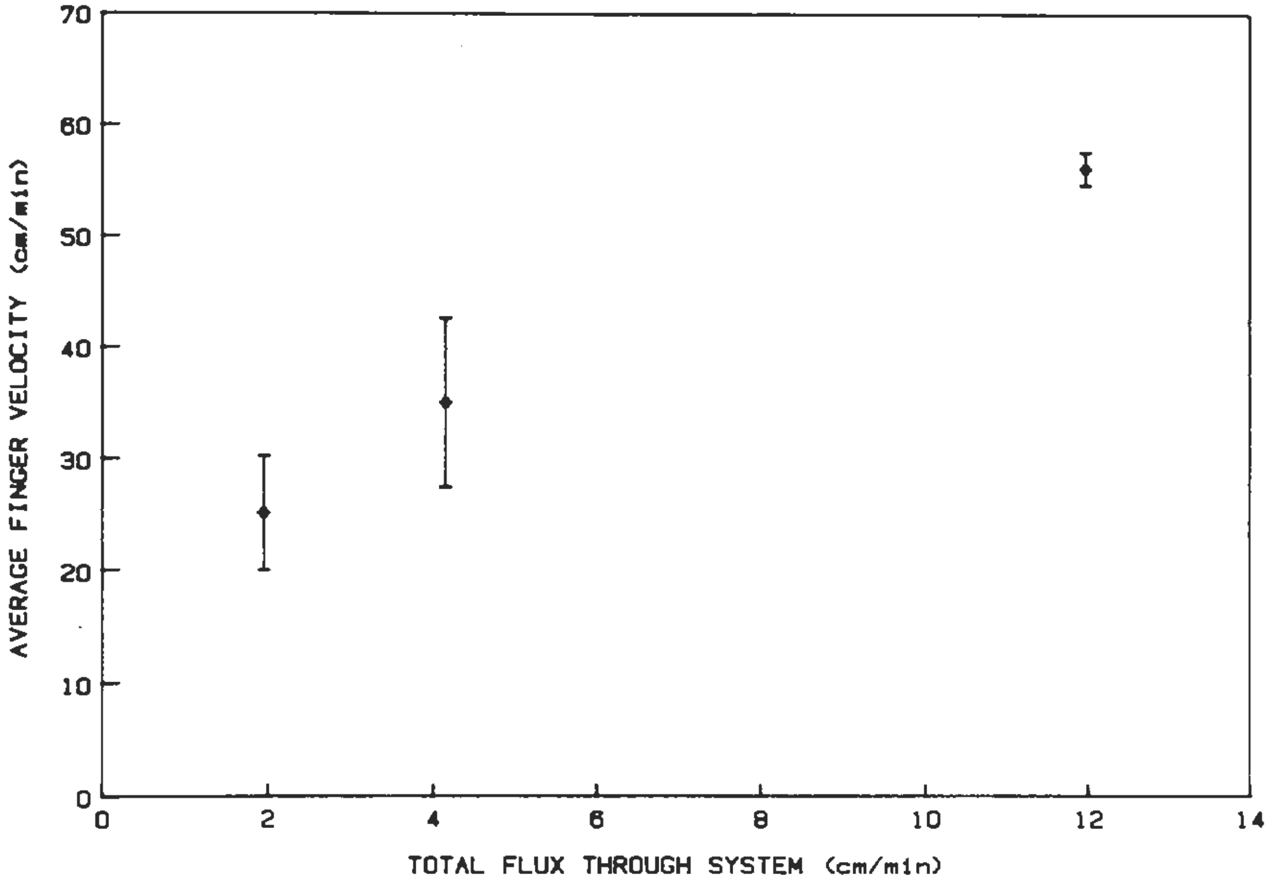

Figure 7. Influence of total flux through the two layer system, Q_T, on finger velocity.

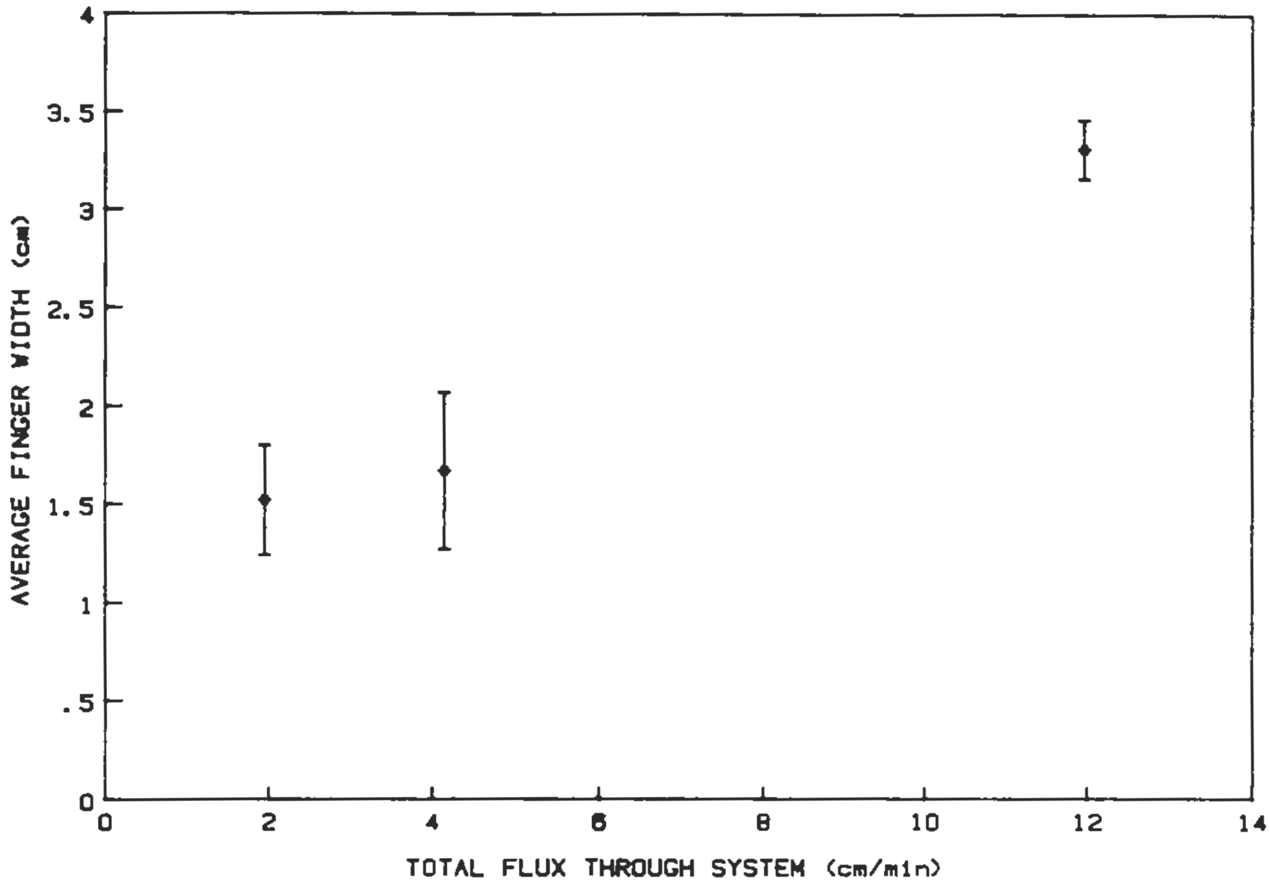

Figure 8. Influence of total flux through the two layer system, Q_T, on finger width.

Table 4. Summary of Point Source Experiments

Run #	Sand Fraction	Porosity (%)	Initial Moisture Content θ_i	Flux Through Finger, Q_f (ml/min)	Finger Velocity (cm/min)	Initial Width (cm)	Boltsman Constant ϕ_f (cm/$\sqrt{min}$)
D7	14-20	42	Dry	10.24	17.85	1.83	.1073
D6	14-20	42	Dry	20.17	30.0	2.43	.1302
D8	14-20	42	Dry	29.88	35.0	3.15	.1061
D4	14-20	42	6%	10.68	6.17	10.1	-
D3	14-20	42	6%	20.0	10.14	11.5	-
D2	14-20	42	6%	30.5	13.33	13.2	-

In the experiments where the initial moisture content is uniform and at field capacity (6%), the flow pattern for point source discharge is qualitatively similar to the two layer experiments with the same degree and distribution of initial moisture content (see Figure 9b). No well defined core area is present, the "fingers" are much wider and have a much lower velocity than in the initially dry cases. Lateral movement is much enhanced as is the importance of downward movement due to gravity at all distances from the middle of the finger.

Lateral Movement of Water from Finger Core

Lateral movement is due to capillary forces and is analogous to infiltration in a horizontal column. In order to quantify lateral movement, the Boltsman constant, ϕ_f, is calculated for each time that the lateral wetting front is drawn using a region of the finger that is the least effected by the downward moving bulges at the sides of the fingers. These values are shown in Table 4.

The Boltsman constant is simply the distance to the wetting front divided by the square root of the time from the start of lateral diffusion. For horizontal (lateral) infiltration with a step change in the moisture content at $x = 0$ to some value θ_o which does not vary in time, ϕ_f is a constant and dependent on θ_o. The Boltsman variable increases with θ_o until it reaches a maximum value when θ_o is the saturated moisture content. For the 14-20 sand with θ_o at saturation, ϕ_f is found to be 23.71 cm/$\sqrt{min}$. Comparison with values for ϕ_f calculated from fingers indicates that the moisture content at the supply surface for lateral diffusion is substantially less than saturation.

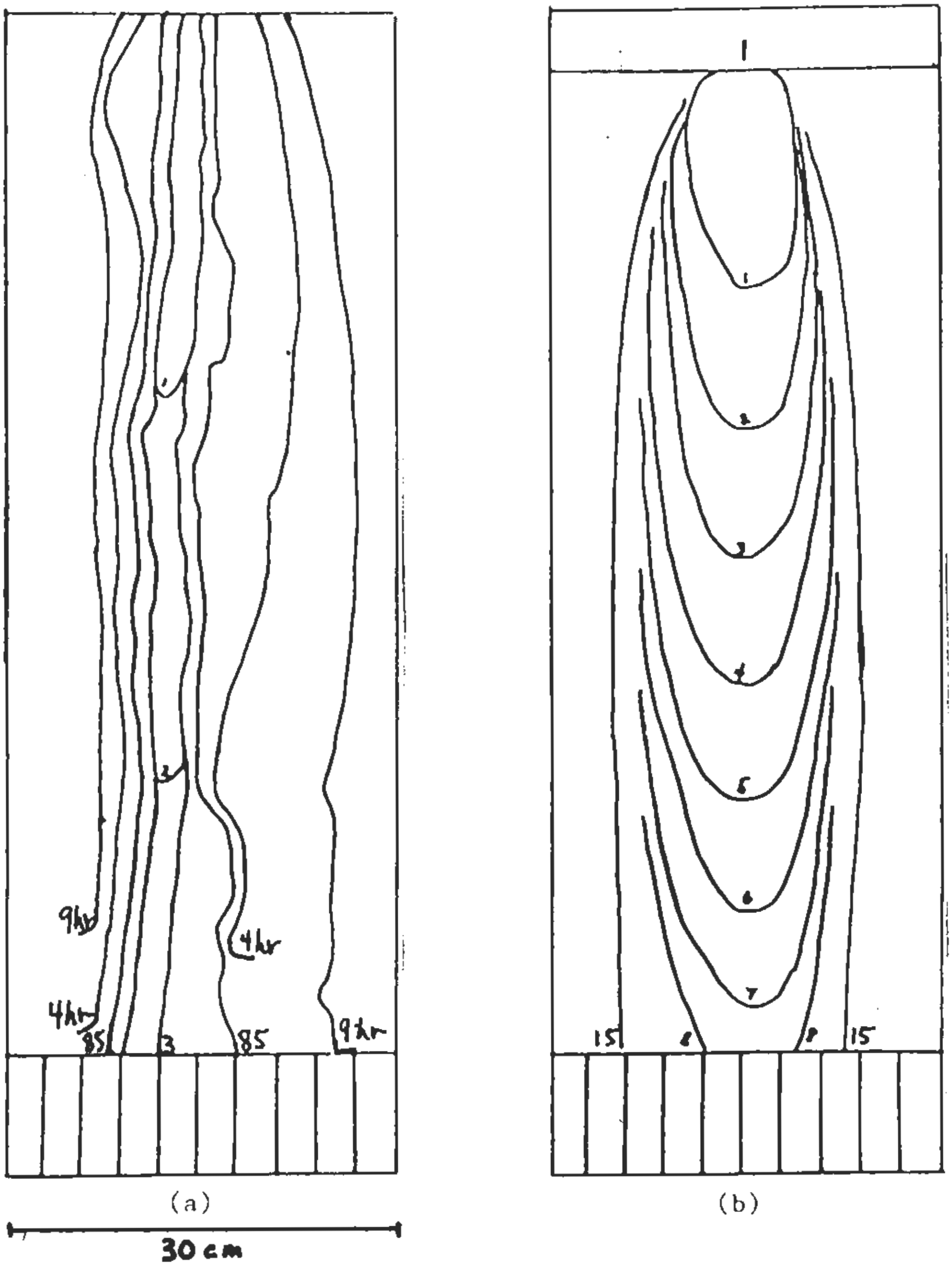

(a) (b)

Figure 9a. Wetting front position for various times (minutes), from a point source (Q = 20 ml/min) located at the top of an initially dry, single coarse layer (14-20 fraction).

Figure 9b. Wetting front position for various times (minutes), from a point source (Q = 20 ml/min) located at the top of a single coarse layer (14-20 fraction) with a uniformly distributed initial moisture content of 6% (field capacity).

PROPERTIES OF INDIVIDUAL FINGERS IN INITIALLY DRY MEDIA

Fingers from all initially dry two layer and point source experiments are considered in order to determine the properties of individual fingers such as their width and velocity, in relation to the porous media properties and the flux feeding a finger. All fingers which neither run down the edges of the chamber nor interact with other fingers are included.

Relationship Between Velocity and Width of Fingers

Figure 10 is a plot of finger width vs. finger velocity. Each point represents an individual finger; the porous media type is designated by the character at the point. It is evident that there is a positive relationship between the finger width and the velocity in a particular porous medium, the higher the velocity, the greater the width.

Fingers from experiments A6a, A8a and A9a show this relationship well. All the fingers from these experiments seem to fall on a straight line. On the other hand, it is also understandable, indeed highly probable, that there is a lower non-zero limit to the width of a finger in a particular porous media. This conjecture is supported by observations on dendrites which often formed during the course of an experiment. These are not included in the figures or summary tables, however, none of these had widths less than .8 cm and yet often their velocities were on the order of 1 cm/min or less.

It also seems reasonable to extend the line in Figure 10 to approach the maximum velocity that a finger could obtain and then level off since the velocity could no longer increase but the width would. Thus at low and at high velocities relative to the maximum finger velocity, the width and velocity of a finger are probably not related one to one.

It is possible that the way a finger originates may also have an effect on it velocity and width. All of the fingers generated by a stream from a burett lie below the line made by fingers from A6a, A8a and A9a. The only difference between the point source and these experiments is the way the finger is generated, one from an instability at a textural interface and the other from a stream of water. The high velocity stream could be deflected by individual grains and made to spread out even though a small cotton ball is used to absorb most of the kinetic energy of the stream. Thus, it is hypothesized that the stream from the burett was strong enough to effectively widen the "point" source to an area source. This area source, if larger than that supplying a finger at a textural interface, could well generate a wider finger and thus with a lower velocity for the same supply flux.

The grain size of the porous media is seen to be a major factor in the velocity vs. width relationship. Twelve fingers in bottom layers other than the 14-20 sand were observed from experiments A5a (20-30 sand), Pre3, A2, and A7a (40-50 sand), and are shown in Figure 10. The general shape of the velocity vs. width relationship is the same,

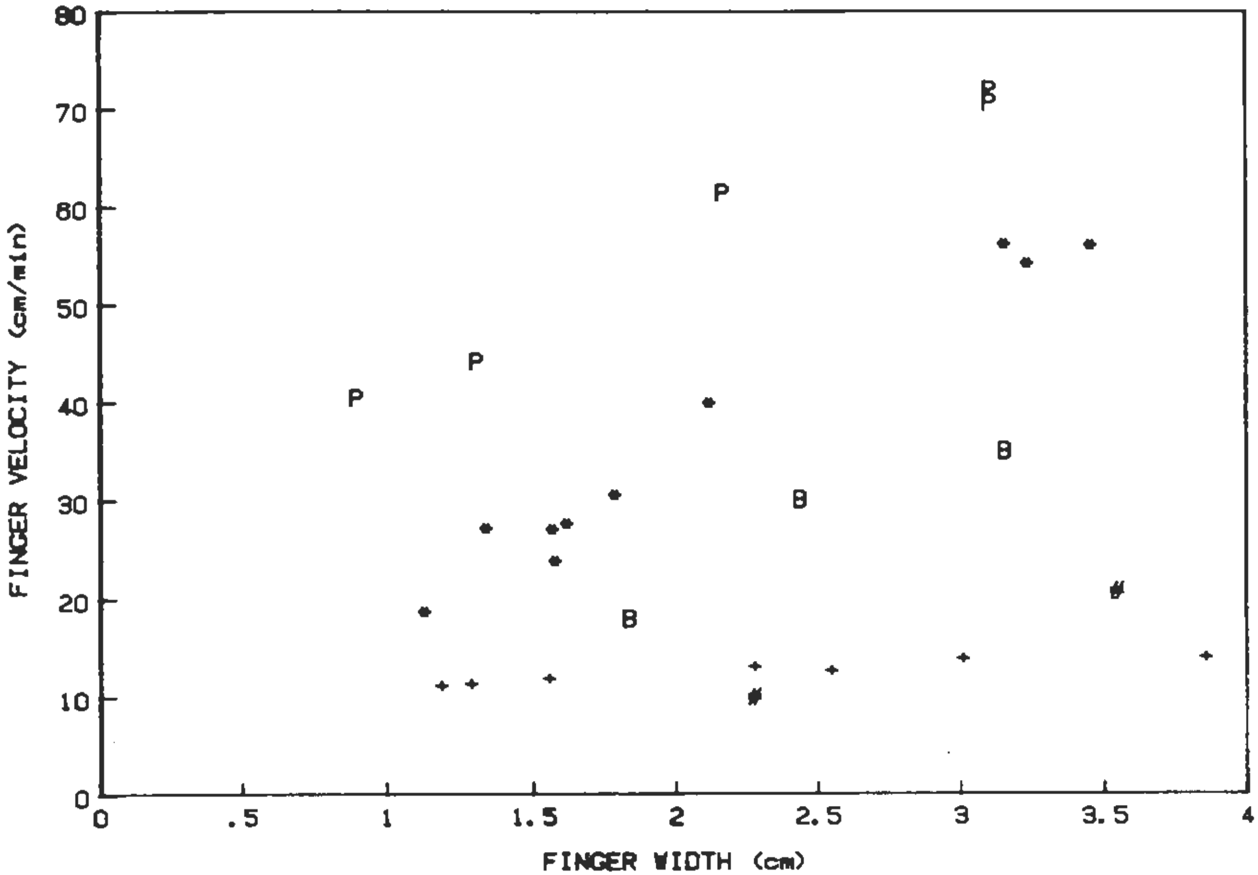

Figure 10. Relationship between finger width and finger velocity. Each point represents an individual finger. Porous media type is given by the characters: * denotes 14-20 sand; # denotes 20-30 sand; P denotes 14-20 pre-cleaned sand; + denotes 40-50 pre-cleaned sand; and B denotes point source experiments conducted in 14-20 sand.

however, the endpoints should change. From these results it is hypothesized that the low end of the graph will show limiting widths that increase as mean grain size decreases and the high end will show limiting velocities that decrease as the mean grain size decreases.

The effect of contact angle on the velocity vs. width relationship can be seen in both the 14-20 sand and the 40-50 sand. Experiments Pre2 and Pre3 conducted on dirty, prewashed sand fall on lines above those for the washed sands (see Figure 10). The dirty sand has a non-zero contact angle and is thus more hydrophobic than the clean sand. This leads to the narrowing of a finger and thus an increase in the initial moisture content in the core. A higher moisture content translates to a higher velocity since the conductivity increases with moisture content.

Individual Finger Properties as a Function of the Flux through a Finger

In initially dry two-layer experiments A6a, A8a and A9a, it was possible to measure the flux through individual fingers, Q_F. Figures 11 and 12 are plots of the flux through a finger, Q_F, versus the velocity and width of the finger respectively. These figures show that increasing Q_F increases both finger velocity and width. This result can also be inferred from Figures 7 and 8 with the finding that an increase in the total flux through the system does not lead to an increase in the number of fingers that form.

Figure 13, a plot of the product of finger velocity and finger cross-sectional area versus Q_F, shows almost a linear function between these two. The relationship between the moisture content of the finger core, θ_c and Q_F can be extrapolated from this plot if the finger moisture content structure is approximated by a step function, equal to zero outside the finger and to some constant value θ_c inside the finger. This approximation is good for dry coarse porous media where the diffusivity approaches a delta function and thus the wetting front approaches a step function in moisture content (Philip 1969). Q_F is then equal to the product of the cross-sectional area of the finger, θ_c, and the macroscopic pore velocity (Darcy scale). If the velocity of a finger is taken as the pore velocity then θ_c may be found by dividing Q_f by the product of finger velocity and finger area. Figure 13 shows that the relationship between Q_F and the product of finger velocity and area is approximately linear and has a positive y intercept. This linear function may not be valid outside the range of experimentally determined values (i.e., Q_F below 6 and above 75 ml/min). Since the y intercept is positive, the moisture content within the core of a finger increases as the flux through the finger increases. This relationship is also substantiated by Figure 11 since the conductivity and thus the finger velocity is a function of θ and so an increase in finger velocity implies an increase in θ_c.

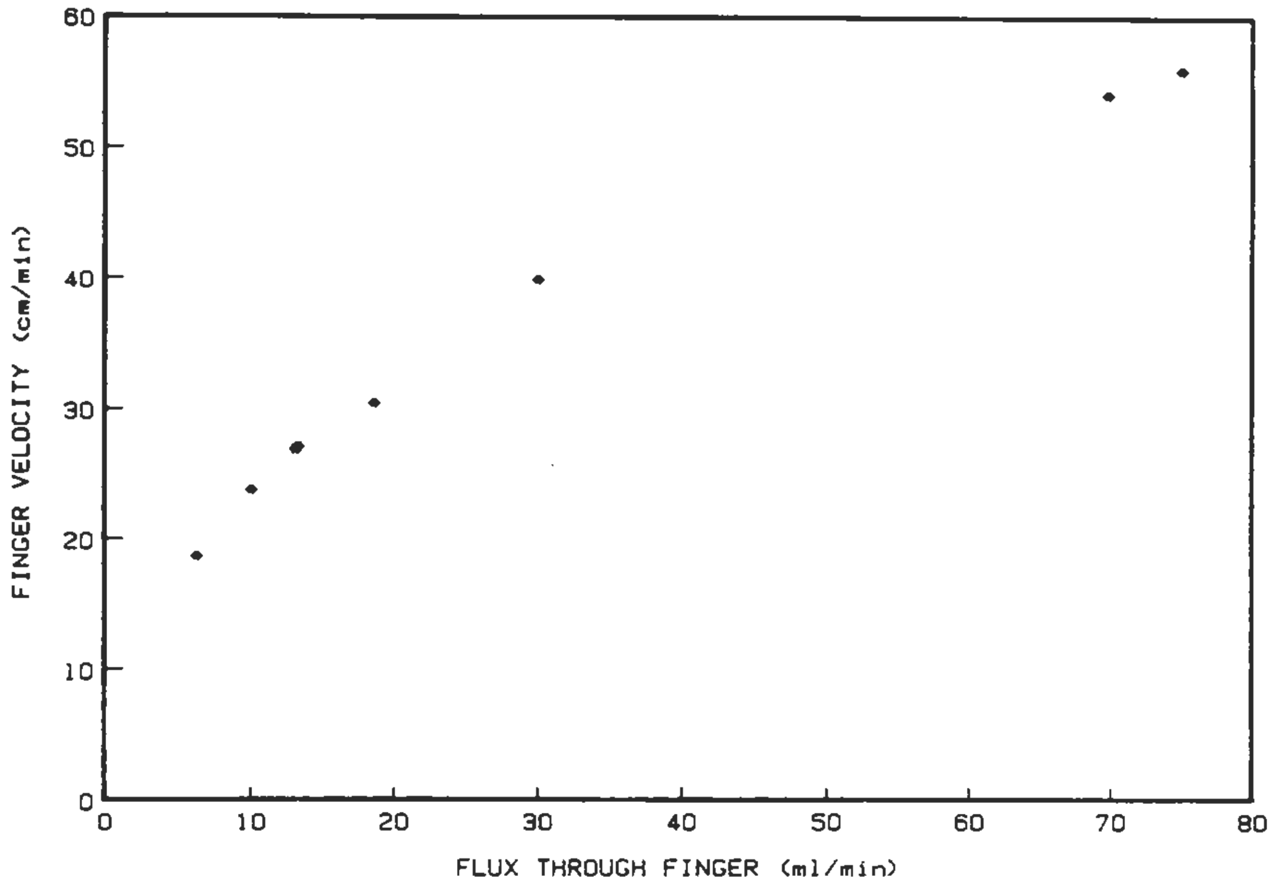

Figure 11. Plot of finger velocity versus the flux through the finger.

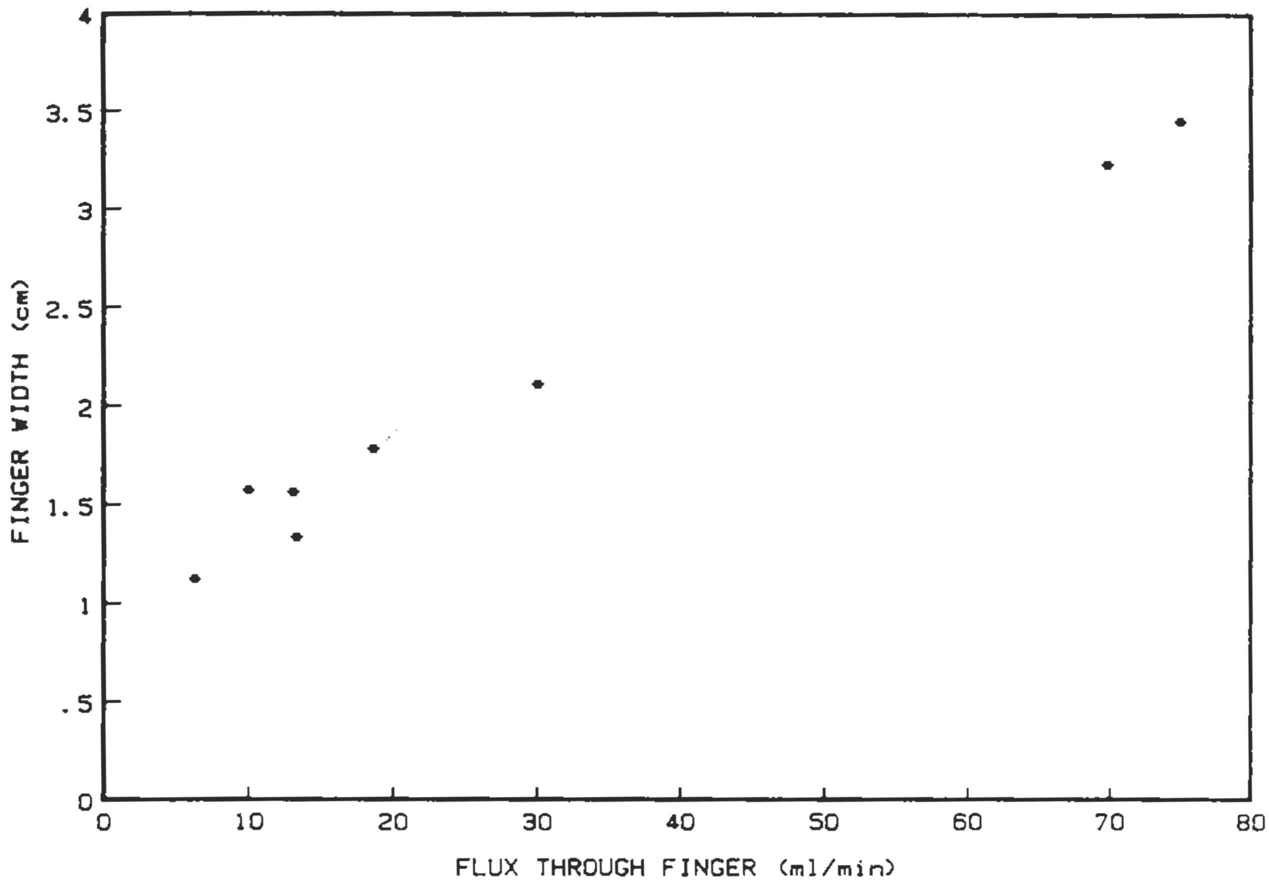

Figure 12. Plot of finger width versus the flux through the finger.

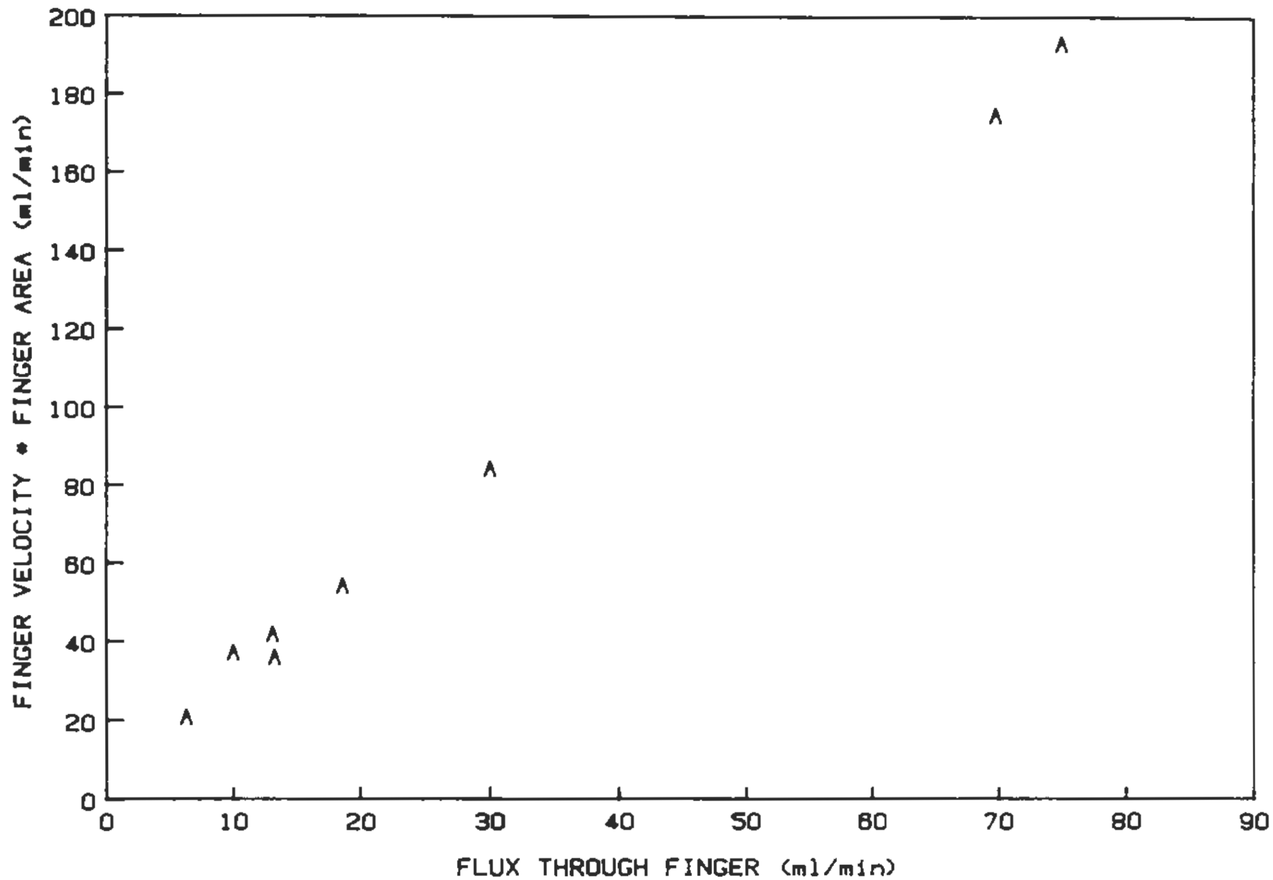

Figure 13. Plot of finger velocity times cross-sectional area versus the flux through the finger.

CONCLUSIONS

Laboratory apparatus and procedures for the study of wetting front instability were developed and two laboratory experimental sets were completed that increased the understanding of the phenomenon.

From the results of these experiments it is concluded that:

1) wetting front instability may occur under a wide range of conditions where the top soil has a lower conductivity than the subsoil;

2) high initial moisture contents, while having a stabilizing effect when uniformly distributed, allow instability to occur when it is distributed heterogeneously by an earlier unstable infiltration flow;

3) unstable flow fields, once established, change very little in time even over relatively long lengths of time with continuous flow (ten days); and

4) average finger width and velocity in the two-layer systems are functions of at least the total flux through the system and the porous media properties of grain size and contact angle;

5) in a particular porous medium, individual finger width, velocity and core moisture content all increase with an increase in the flux through the finger.

The results of this study have implications for monitoring systems and groundwater pollution prediction models applied to field soils where instability occurs. This study has demonstrated that the phenomenon is important and most likely as widespread as Hill and Parlange (1972) state. This study has also demonstrated that unstable flow fields and finger properties may be systematically and quantitatively explored through controlled laboratory experimentation.

Laboratory experimentation is underway to further substantiate and generalize the findings of this study to a wide variety of porous media. Field experimentation has also begun and the results of a preliminary field experiment indicate the occurrence of fingering at Cornell University's Horticulture Research Farm on Long Island.

The study of wetting front instability must continue so that it may be fully understood and thus allow the formulation of predictive equations. The present study has formed a sound basis on which future work will build.

REFERENCES

Bodman, G.B. and E.A. Colman. 1943. Moisture and energy conditions during downward entry of water into soils. Soil Sci. Soc. Am. Proc. 8:116-122.

Diment, G.A. 1982. Analysis of wetting front instability in unsaturated porous materials. Unpublished Ph.D. thesis, University of New South Wales, Australia.

Dixon, R.M. and A.E. Peterson. 1971. Water infiltration control: A channel system concept. Soil Sci. Soc. Am. Proc. 35, 398-973.

Ehlers, W. 1975. Observations on earthworm channels and infiltration on tilled and untilled loess soil. Soil Sci. 119:242-247.

Elrick, D.E. and L.K. French. 1966. Miscible displacement patterns on disturbed and undisturbed soil cores. Soil Sci. Soc. Am. Proc. 30:153-156.

Germann, P. and K. Beven. 1981. Water flow in soil macropores. Soil Sci. Soc. Am. J.

Hill, D.E. and J.Y. Parlange. 1972. Wetting front instability in layered soils. Soil Sci. Soc. Am. Proc. 36:697-702.

Lawes, J.B., J.H. Bilbert and R. Warington. 1882. On the amount and composition of the rain and drainage waters collected at Rothamsted. William Clowes and Sons, LTD. London. Quoted by Thomas and Phillips (1979).

Parlange, J.Y. and D.E. Hill. 1976. Theoretical analysis of wetting front instability in soils. Soil Sci. 122:236-239.

Philip, J.R. 1969. Theory of infiltration. Adv. Hydrosci. 5:215-296.

Philip, J.R. 1975a. Stability analysis of infiltration. Soil Sci. Soc. Am. Proc. 39:1042-1049.

Quisenberry, V.L. and R.E. Phillips. 1976. Percolation of surface applied water in the field. Soil Sci. Am. J. 40:484-489.

Russo, D. and E. Bresler. 1981. Effect of field variability in soil hydraulic properties on solutions on unsaturated water and salt flows. Soil Sci. Soc. Am. J. 45:675-681.

Saffman, P.G. and G.I. Taylor. 1958. The penetration of a fluid into a porous medium or Hele-Shaw cell containing a more viscous liquid. Proc. Roy. Soc. Ser. A 245:312-331.

Starr, J.L., H.C. DeRoo, C.R. Frink and J.Y. Parlange. 1978. Leaching characteristics of a layered field soil. Soil Sci. Soc. Am. J. 42:386-391.

Thomas, G.W., R.L. Blevins, R.E. Phillips and M.A. McMahon. 1973. Effect of hilled sod mulch on nitrate movement and corn yield. Agron. J. 65:736-739.

Thomas, G.W. and R.E. Phillips. 1979. Consequence of water movement in macropores. J. Environ. Quality 8:149-152.